A Study on the Sealing Gaps of Internal Gear Ring Pumps for Automotive Drivetrain Applications

Dipl.-Ing. Wolfgang Schweiger, Dipl.-Ing. Werner Schoefmann

MAGNA Powertrain, Industriestraße 35, 8502 Lannach, Austria, E-mail:
wolfgang.schweiger@magnapowertrain.com, werner.schoefmann@magnapowertrain.com

Ass.-Professor Dr.-Ing. Andrea Vacca

Maha Fluid Power Research Center, Purdue University
1500 Kepner Drive, Lafayette, IN, USA, E-Mail: avacca@purdue.edu

1 Abstract

This paper presents the latest effort made by the authors in the development of a comprehensive modeling approach useful for the design and analysis of internal gear ring pumps. In particular, the present work focuses on the radial and lateral sealing gap modeling. A CFD model for the accurate evaluation of lateral leakages and shear stresses has been coupled with a lumped parameter fluid dynamic model, which is used to simulate the main flow through the unit. Radial leakages at tooth tips are modeled through a lumped parameter orifice model based on a deep evaluation of variable gap geometry. The results presented in this work demonstrate how the developed tool can be used to gain knowledge about the operation of internal gear pumps with high level of details as concerns the features of internal flow.

KEYWORDS: gear ring pump, gerotor pump, internal and external leakage, lateral and radial sealing gaps, multi domain simulation approach

2 Introduction

In many automotive fluid power applications gear ring pumps (GRPs) are a preferred solution because of their small package size, low manufacturing costs and robustness. Their range of operation is usually limited by the reduction of pump efficiency at higher pressure levels due to the functionally necessary sealing gaps. Sealing gap tolerances have large practical implications in both steady-state and dynamic pump operation as well as in the manufacturing costs. The present work aims to advance the current understanding of the effects related to the lubricating gap flow and to the geometric tolerances on the pump performance.

Reference applications are automotive drivetrain applications, where the pump can be used at different operating conditions. One main application is the use of transmission pumps for torque control in all-wheel-drive systems. The main purpose of this application is to generate pressure in response to a differential speed between the left and right wheels or between the front and rear axle of a vehicle. The pressure actuates a clutch to reduce the speed difference. In this application, the pump operates at very low speeds. However, in other applications, such as lubricating oil pumps or electrical oil pumps, the pump is used to lubricate, to cool or to actuate the various components of the transmission and then the pump operates at very high speeds (800 - 8000 rpms).

Traditionally, GRP designs are a result of mainly empirical processes, strongly influenced by the experience acquired by pump manufacturers. Therefore, extensive and time consuming experimental activity is required to investigate the effect of each design parameter and the geometrical tolerances on the pump operation. Current simulation models, like /1-3/, only focus on limited aspects of operation, and in particular do not consider details regarding the simulation of the sealing gaps. Different studies on other positive displacement machines, like external gear machines /4,5/, or axial piston machines /6,7/, show the crucial importance of these gaps in the operation of the unit. A first step towards an omni-comprehensive modeling approach for GRPs has already been presented by the authors in a previous work /8/. However, this work was limited to an accurate prediction of the main flow through the unit accounting for a deep evaluation of the geometric features of the GRP, but strong approximations were made as concerns the leakage flows and the evaluation of shear stress dissipation at the lateral sealing gaps, which are bounded by the rotating gears and the housing. The purpose of the present study is the numerical investigation of the effect of these lubricating gaps in GRPs.

The operating principle of a GRP can be described by use of **Fig. 1** as a positive displacement mechanism which moves the oil due to the displacing action, which is caused by the rotation of the gears, from the suction port to the delivery port. The pump is composed of a rotor set, comprising an inner and an outer rotor and a housing which usually consists of three parts: a mid plate, a base plate and a cover plate. As the inner rotor rotates, it gets into contact with the outer rotor and consequently the outer rotor is driven by the inner rotor motion. Due to the eccentricity e between the inner and outer rotor axis, displacement chambers between the inner and outer gears are formed. The displacement chambers are sealed to adjacent chambers by radial sealing gaps and to the housing by lateral sealing gaps. During one revolution of the outer rotor, the displacement chamber gets a maximum and minimum volume. The teeth contact starts around the Bottom Dead Center (BDC in Fig. 1) where the minimum chamber value occurs. As the rotors continue to rotate, the chamber volume increases until it reaches its maximum value at Top Dead Center (TDC in Fig. 1). This side of the pump is connected to the suction port (low pressure side). After crossing the Top Dead Center, the chamber volume is decreasing. This side of the pump is connected to the delivery port (high pressure side). The original approach presented in this work allows a detailed study of the internal and external leakage flow as well as the influence of the gap parameters on the complete pump assembly.

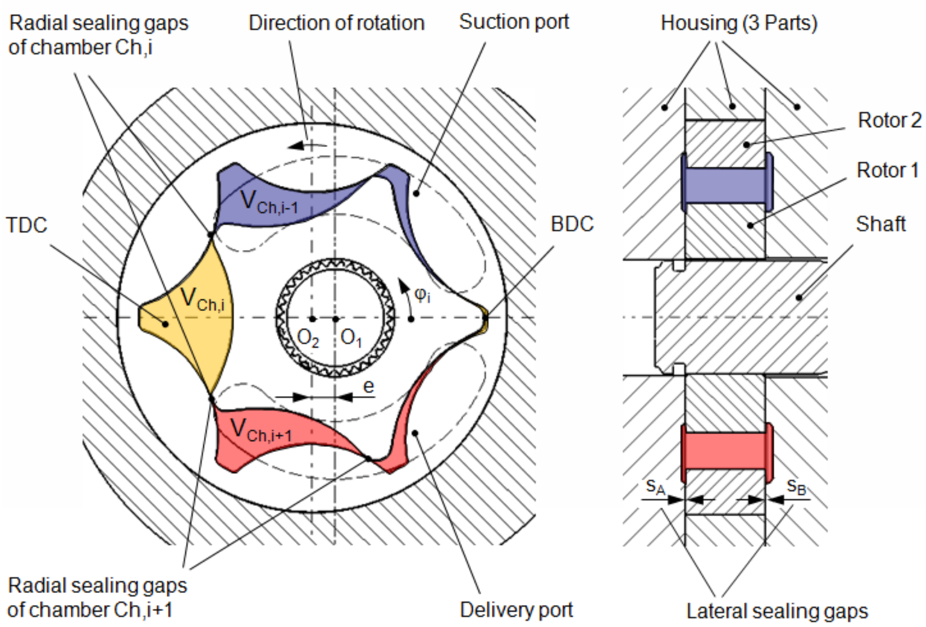

Figure 1: Internal gear ring pump

3 Modeling Approach

This work takes as reference the basic modeling approach described by the authors in /8/. This approach comprises submodels which are interacting in different domains and it has been supplemented with an additional CFD submodel. The respective models and the data flow are presented in **Fig. 2**. All essential pre- and post-processing operations can be performed out of a global graphical user interface which controls the models and their interactions. It enables access to relevant design and simulation parameters, used in different domains of the simulation procedure. The geometric model generates the gear profiles based on trochoidal curves and their conjugates as well as the porting geometry, which is controlled by a few basic design parameters. Alternatively, coordinates obtained from measured data or CAD data can be used, due to an integrated geometry import/export facility, for consideration of modified teeth shapes or more complex porting geometries. More details about the geometric model are reported in /8/. The lumped parameter fluid dynamic model describes the flow through the GRP due to displacement action. Each displacement chamber $V_{ch,i}$ in Fig. 1 is considered as a separate control volume and its pressure is assumed uniform and only depends on time according to Eq. 1.

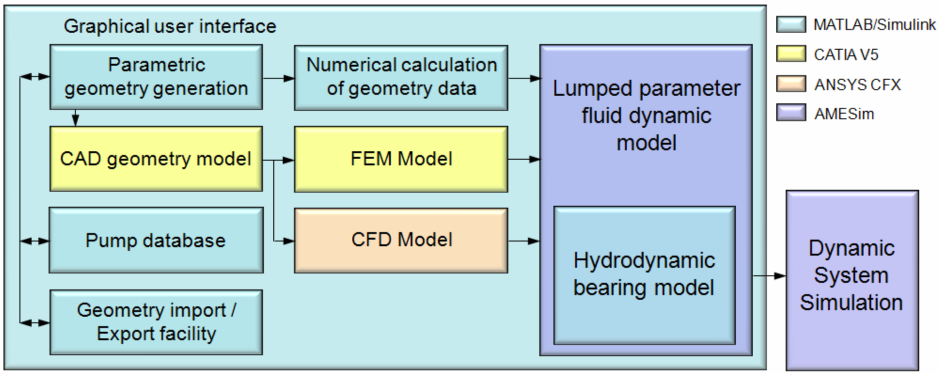

Figure 2: Modeling Approach

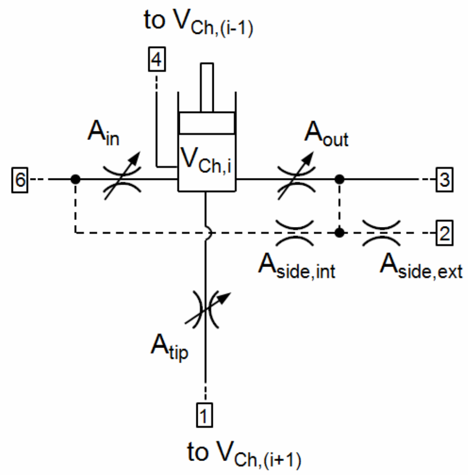

Fig. 3: Schema of the fluid dynamic model showing connections of a single displacement chamber

$$\frac{dp_i}{d\varphi} = \frac{\beta}{\rho_i} \frac{1}{V_{Ch,i}\varpi_1} \left(\sum \dot{m}_j - \varpi_1 \rho_i \frac{dV_{Ch,i}}{d\varphi} \right) \qquad (1)$$

Figure 3 shows an equivalent cylinder-piston representation of a single displacement chamber $V_{ch,i}$ which is connected to the suction and delivery port by equivalent orifices, representing the inlet and outlet porting geometry (A_{in}, A_{out}). These features are automatically evaluated by a geometric model. Furthermore, each contol volume is connected to its adjacent chamber volumes and to the drain by orifices, representing the leakage paths for the radial and lateral leakage flow due to clearances (A_{tip}, $A_{side,int}$, $A_{side,ext}$). These clearances are acting as sealing gaps and affect the pump performance with their variable height, length and width of the leakage path. Therefore an accurate description of the effective sealing gap geometry - which continuously changes with the angular position of the gears - is required and the respective models are described in the following sections.

3.1 Model for the lateral sealing gaps

The flow in the lateral sealing gaps is evaluated through a 3D CFD simulation approach. The CFD model is realized in ANSYS, with a numerical solver based on Navier-Stokes equations. The simulation domain is obtained through an automatic mesh generation process fully integrated in the simulation model, as shown in Fig. 2. This enables the calculation of the pressure distribution in the lateral sealing gaps between the rotor assembly and the housing, considering full hydrodynamic lubrication.

The simulation domain - the effective lateral sealing area which enables a lateral leakage flow - is generated by a 3D CAD geometry model with a proper angular step and a resolution of 36 degrees is used for the results presented in this work. The relevant domains are discretized into a finite element volume mesh comprising of hexahedron elements. **Figure 4** shows the mesh for 2 positions. The model assumes a constant lateral gap height and consists of 5 to 9 layers in lateral direction. A detailed view of the mesh is shown in Fig. 4c and average mesh properties are listed in Table 1.

(a) 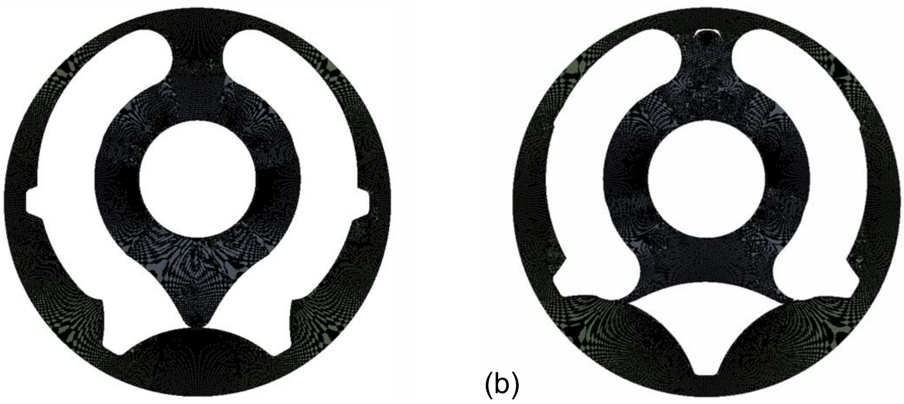 (b)

(c) 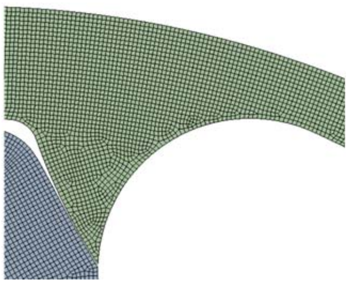

Table 1: Average mesh properties

Element type	Hexahedron
Element size	0.02 mm
Layer in lateral direction	5 … 9
Nodes	83.500
Elements	71.500

Figure 4: (a), (b) Mesh for 2 angular gear positions for a selected reference pump with z_1=5 teeth; (c) Mesh detail

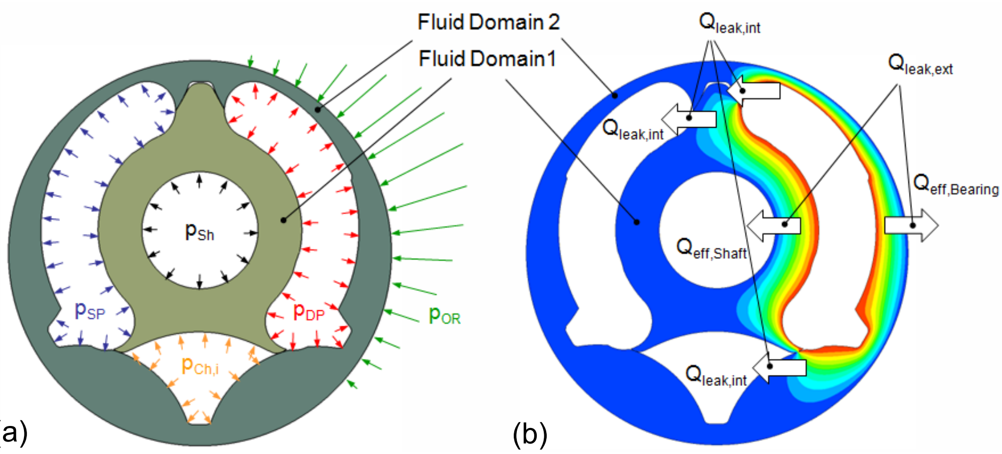

(a) (b)

Figure 5: Computational Domain; (a) pressure boundary conditions along the lateral gap; (b) pressure field in the lateral sealing gap

Figure 5b shows how both the internal and the external lateral leakage flow are evaluated. The external leakage flow is the flow by the outer rotor bearing boundary and the inner rotor shaft boundary, whereas the internal flow is the flow between the high and low pressure ports. The total leakage flow is the total amount of the external and internal leakage flow. It can be determined as total inlet flow into fluid domain 1 and 2 by the delivery port boundaries.

The model also evaluates the torque dissipation due to viscous friction on the lateral surface of the gears. The obtained results for internal and external leakage flow rates and viscous friction torque losses are implemented within the AMESim fluid dynamic model by using look up data tables. The lateral orientation of the gears is not known a priori and can be varied by setting the parameters $\boldsymbol{s_A}$ and $\boldsymbol{s_B}$ as indicated in the cross sectional view of Fig. 1.

3.2 Model for the radial sealing gaps

A radial leakage flow between adjacent displacement chambers is caused by the teeth tip clearance (TC). These connections are taken into account by the laminar flow equation (2) assuming fully developed laminar flow. A numerical model has been developed to accurately consider the influence of the instantaneous gap geometry on the radial leakage flow. The model considers the variation of both the gap height and the gap length as a function of the angular position of the gears. The radial gap height $\boldsymbol{h_r}$ influences the leakage flow rate by the third power and can be determined directly out of the numerical geometry model. In consideration of the gap length, an effective radial sealing gap length $\boldsymbol{l_r}$ has been determined as the shortest distance where the gap height $\boldsymbol{h_r}$ increases by a factor $\boldsymbol{k}$ as it is shown in **Fig. 6**. Concerning the selected reference pumps, a suitable value for this parameter is about 1.02 - 1.05, as this matches well with the experimental results.
The geometrical model also permits to consider an asymmetric distribution where different offset values for inner and outer gears can be used.

$$\dot{m}_{i.j} = \rho\left(\overline{p_{i,j}}\right)\left[-\frac{{h_r}^3 b}{12\eta l_r}\left(p_i - p_j\right)\right] \qquad (2)$$

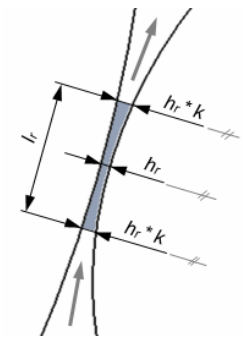

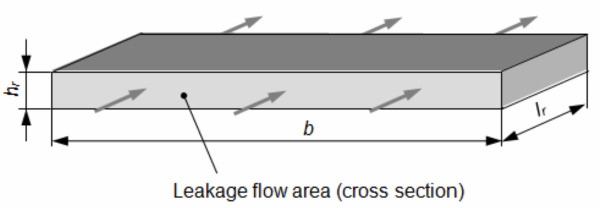

Figure 6: Definition of the radial gap geometry and equivalent orifice model

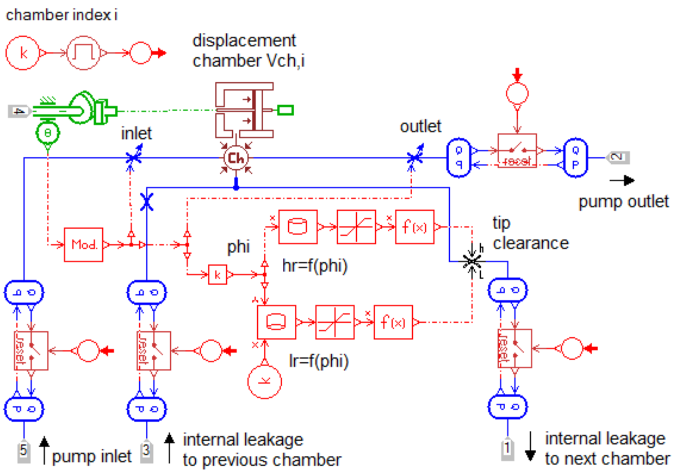

Figure 7: Implementation of the variable radial gap model in AMESim (submodel of a single displacement chamber)

Eq. 2 is used within the fluid dynamic model that evaluates the flow through each displacement chamber, assuming a rectangular gap geometry with constant gap width $\boldsymbol{b}$, variable gap height $\boldsymbol{h_r}$ and variable gap length $\boldsymbol{l_r}$. **Figure 7** displays the model for a single displacement chamber with the implemented tip clearance submodel. To simulate the whole GRP, the model in Fig. 8 is repeated for each displacement chamber of the unit.

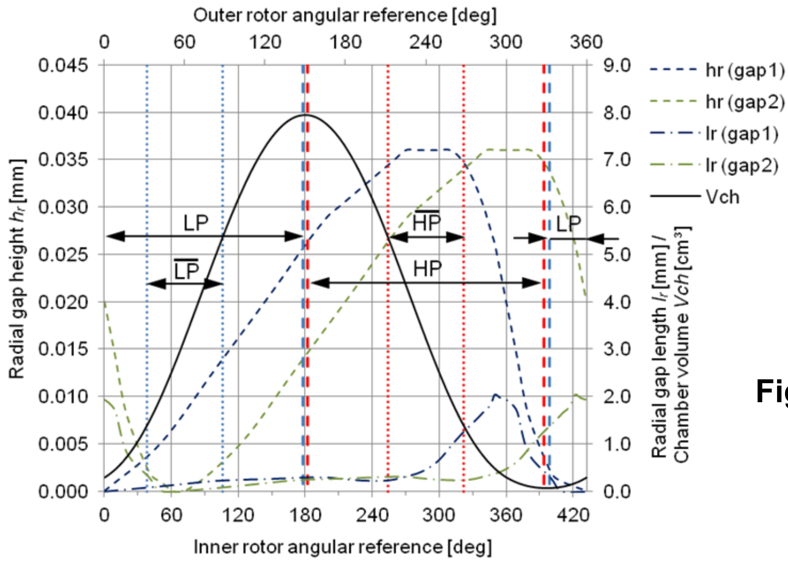

Figure 8: Correlation of chamber volume with radial sealing gap geometry

Figure 8 displays the radial sealing gap height $\boldsymbol{h_r}$ and gap length $\boldsymbol{l_r}$ as function of the angular position of the gears. In this example, a selected reference pump ($\boldsymbol{z_i = 5}$, $\boldsymbol{e = 4mm}$, $\boldsymbol{b = 17mm}$, $\boldsymbol{q_v = 39.5cc}$) as shown in Fig. 1, is taken into consideration and a symmetrical distribution of the nominal tip clearance $\boldsymbol{TC = 0.04mm}$ on the inner and outer rotor geometry is assumed. $\boldsymbol{LP}$ indicates the angular section with low pressure where the displacement chamber is connected to the suction port. Accordingly, $\boldsymbol{HP}$ refers to the corresponding angular section at high pressure, connected to the delivery port. The angular range where the displacement chamber is entirely covered by the suction port and delivery port respectively is indicated with $\overline{\boldsymbol{LP}}$ and $\overline{\boldsymbol{HP}}$. Around bottom and top dead center (BDC, TDC, as defined in Fig. 1), there is a small angular range remaining in the transition zone between LP and HP. The correlation of the chamber volume of the considered displacement chamber with the corresponding sealing gap geometry, occurring between adjacent displacement chambers, has to be taken into account. According to Fig. 8, gap 1 is the sealing gap to the previous displacement chamber and gap 2 is the sealing gap to the following displacement chamber.

4 Results and Experimental Validation

The result section first presents results obtained with the submodels for the lateral and radial sealing gaps for different gap heights and operating conditions. Then, the influence of the implementation of the specific leakage models in the pump performance and a comparison with measured data is shown.

4.1 Results for the lateral and radial sealing gaps

The results obtained with the lateral gap model have confirmed the expected negligible influence of pump speed in the leakage flow and have shown that there is a negligible influence of delivery pressure in the viscous torque. **Figure 9a** displays the expected influence of gap height in the total lateral leakage flow for different oil temperatures and delivery pressures. **Figure 9b** shows a linear relationship between the viscous torque and pump speed for different oil temperatures and gap heights.

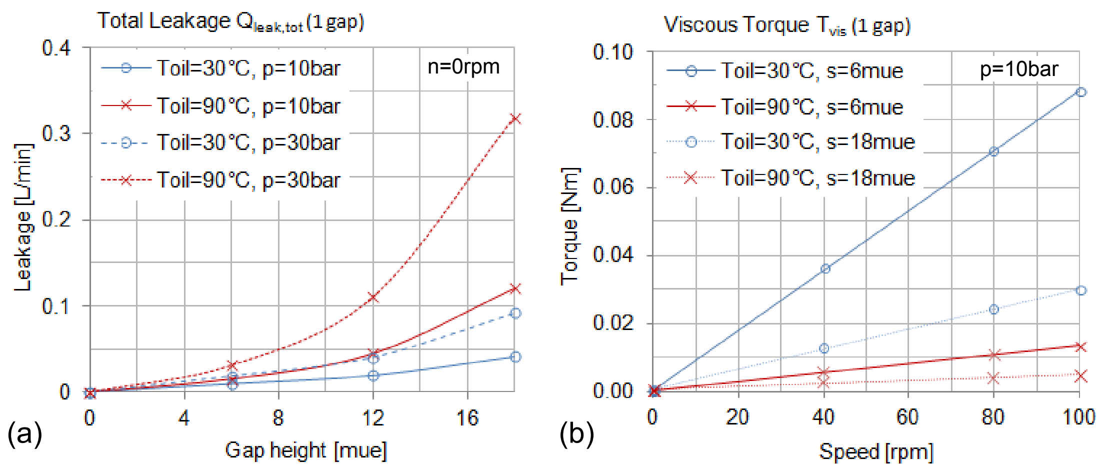

Figure 9: (a) Total lateral leakage flow for different operating conditions and gap heights; (b) Viscous torque

Figure 10 demonstrates the variation of the radial gap height above the angular position of the gears determined by the geometrical model and a comparison obtained with measured rotor profiles. The pump taken as reference (transmission oil pump, Fig. 1) is composed of a 5- and 6-toothed rotor and due to geometrical tolerances of the gear profiles the determined sealing gap is varying.

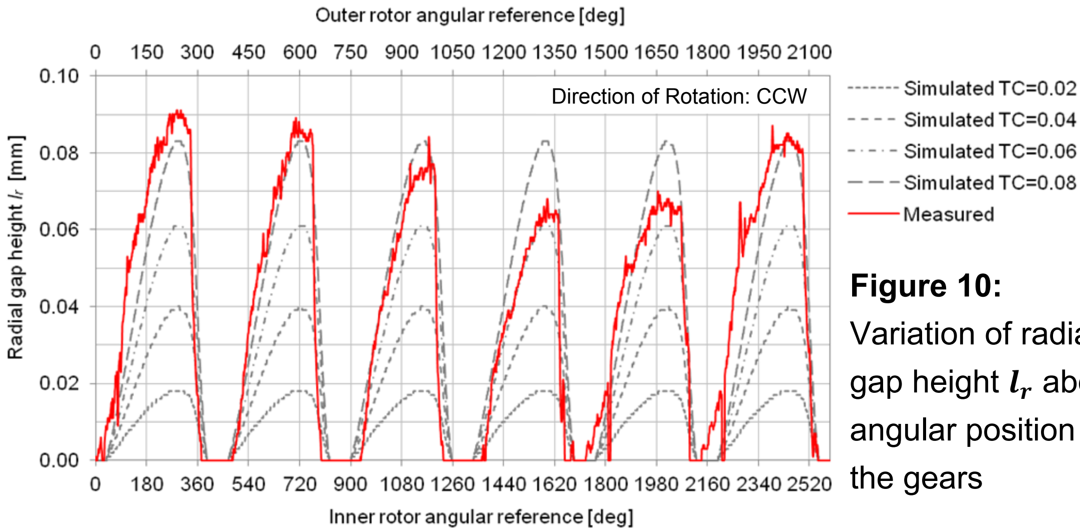

Figure 10: Variation of radial gap height l_r above angular position of the gears

4.2 Results with implemented leakage models

For the purpose of model validation and to quantify the affects of the lateral and radial sealing gap clearances on the pump performance extensive experimental test have been performed. In order to minimize the influence of uncontrolled variables on the test results, one common master housing has been used. Only the rotor assembly was varied in order to achieve the desired values of internal clearance for the lateral and radial sealing gaps.

Figure 11 shows the structure of the pump test bench. It basically consists of a pressure relief valve, a bypass valve and two branches (A, B) used for different measurement purpose, which can be activated selectively by shut-off valves. One branch is restricted by a calibrated orifice and is used for measuring the average discharge pressure and the dynamic pressure ripple at the delivery port. The other branch is restricted by an adjustable throttle valve and is used for measuring the steady state pressure flow characteristic. The oil tank is conditioned by a heating element.

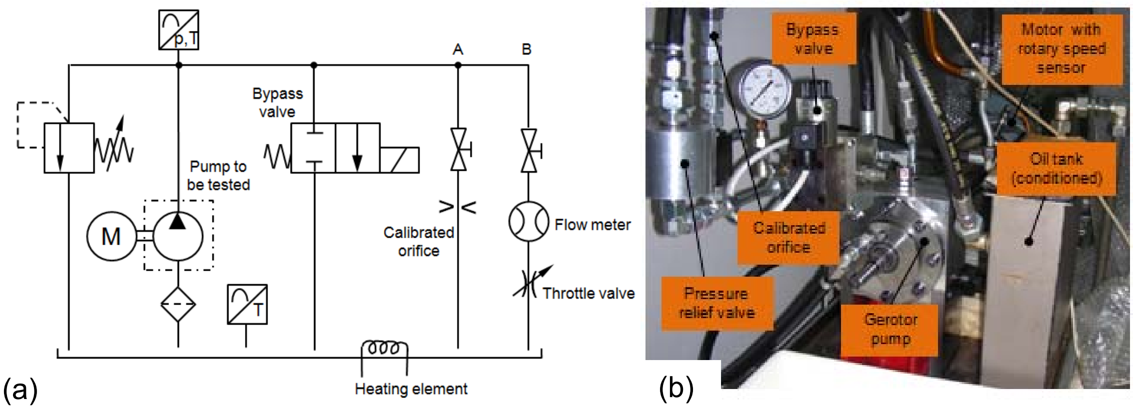

Figure 11: Test bench; (a) Schematic of the hydraulic circuit; (b) Detail view

The models have been validated for different reference pumps and for various discharge pressures, differential speeds and oil temperatures. The simulation results for the selected reference pump (transmission oil pump, Fig. 1) and the correlation with experimental results are shown as an example in **Fig. 12**. 'Sim MIN' and 'Sim MAX' are indicating the simulation results for a pump with minimum and maximum lateral and radial clearance respectively, 'Exp. MIN' and 'Exp. MAX' are indicating the corresponding experimental results.

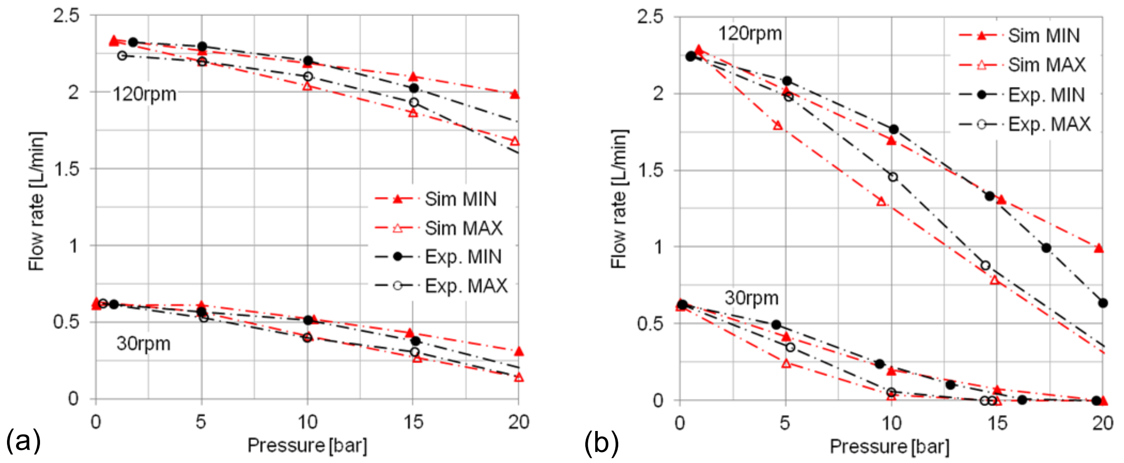

Figure 12: Steady state pressure flow characteristic curves for the considered reference pump; (a) 30°C (b) 70°C oil temperature

Figure 13 gives an insight into internal and external leakage flow rates of the selected reference pump and displays the volume $V_{ch,i}$ of a single displacement chamber and the instantaneous leakage flow in the radial sealing gaps between adjacent displacement chambers. In special gap 1 indicates the flow between the previous chamber and the current chamber, whereas gap 2 indicates the flow between the current and the next chamber.

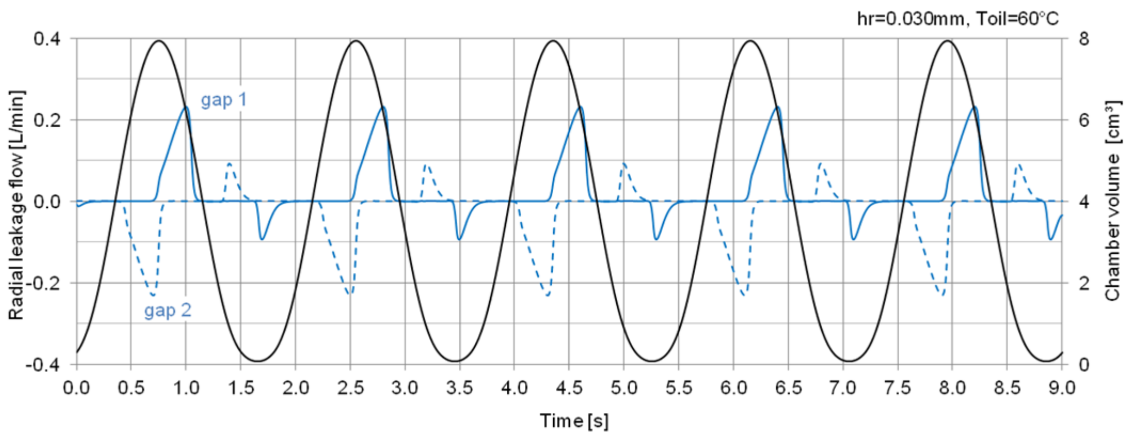

Figure 13: Instantaneous chamber volume and radial leakage flow between displacement chambers

Figure 14a shows the influence of the oil temperature in the radial leakage flow and Fig. 14b displays the influence of the lateral sealing gap height in the external lateral leakage flow as defined in Fig. 5b.

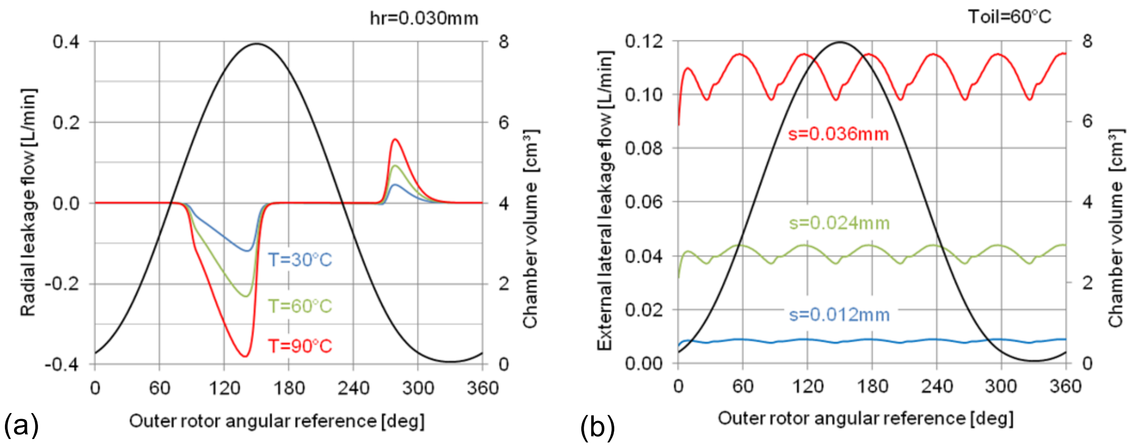

Figure 14: (a) influence of oil temperature in the radial leakage flow; (b) influence of gap height in the lateral leakage flow

5 Summary/Conclusion

While previous work mainly focused on the modeling of flow through the GRP due to displacing action, this work emphasizes on the modeling of the leakage paths due to sealing gaps and shows the influence of the implementation of detailed models for the calculation of the lateral and radial leakage flow in the overall pump performance.

Appropriate and validated models, suitable for the consideration of the features of the lateral and radial leakage flow, based on an accurate description of the gap geometry, have been presented. For the lateral leakages a CFD approach has been used, enabling a detailed analysis of internal and external leakage flow as well as the pressure distribution in the sealing gap and the torque dissipation due to viscous friction. For the features of the radial leakage flow the lumped parameter approach has been followed and a simplified equivalent orifice model has been used. But this is based on solid considerations and a geometrical model for an accurate description of the effective sealing gap geometry has been developed. As it can be seen in the result section, with the presented modeling approach it was possible to reach an acceptable correlation with measured data concerning the overall pump performance for different tolerance combinations (minimum and maximum clearance pump) in the whole range of operation, although there are still effects which are not taken into consideration by the current level of detail (e.g. force balance on moving parts).

6 References

/1/ Fabiani M., Mancò S., Nervegna N., Rundo M., Armenio G., Pachetti C., Trichilo R. "Modelling and Simulation of Gerotor Gearing in Lubricating Oil Pumps", SAE Paper 1999-01-0626, March 1999.

/2/ Neyrat S., Orand N., Jonquet D. "Modelling and Analysis of an Automatic Transmission Internal Gear Oil Pump with Cavitation", SAE Paper 2005-01-2448, May 2005.

/3/ Gamez-Montero P. J. et al. "GEROLAB Package System: Innovative Tool to Design a Trochoidal-Gear Pump", Journal of Mechanical Design, Vol. 131, July 2009.

/4/ Vacca A., Dhar S., Opperwall T. A coupled lumped parameter and CFD approach for modeling external gear machines. 12th Scandinavian International Conference on Fluid Power. 2011.

/5/ Zecchi M., Vacca A., Casoli P. 2010. Numerical analysis of the lubricating gap between bushes and gears in external spur gear machines. PTMC2010 Power Transmission and Motion Control, September 13-15, University of Bath, England.

/6/ Gels S., Murrenhoff H. Simulation of the Lubricating Film between contoured piston and cylinder. International Journal of Fluid Power, Vol. 11 (2010), No. 2

/7/ Wieczorek U., Ivantysynova M. 2002. Computer Aided Optimization of Bearing and Sealing Gaps in Hydrostatic Machines - The Simulation Tool CASPAR. International Journal of Fluid Power, Vol. 3 (2002), No.1, pp. 7-20.

/8/ Schweiger W., Schoefmann W., Vacca A. 2011. Gerotor Pumps for Automotive Drivetrain Applications: A Multi Domain Simulation Approach. Commercial Vehicle Engineering Congress, September 2011, Chicago, IL, USA.

7 Nomenclature

ω	Angular velocity	rad/s	l_r	Radial sealing gap length	mm
p	Pressure	bar	k	Coefficient defining change of gap height	-
$\dot{m}_{i.j}$	Mass flow rate	kg/s			
$\rho(\overline{p_{i,j}})$	Density	kg/m³	V_{Ch}	Chamber volume	cm³
β	Bulk modulus	Pa	b	Rotor width	mm
η	Dynamic viscosity	Pa s	e	Eccentricity	mm
T, $Toil$	Oil temperature	°C	s, s_A, s_B	Lateral sealing gap height	mm
TC	Tip clearance	mm	Q	Volume flow rate	l/min
h_r	Radial sealing gap height	mm	T_{visc}	Viscous friction torque	Nm

Additional Subscripts

CCW	Counter-clockwise rotation	SH	Shaft side
$leak$	Leakage flow	OR	Outer rotor side (outer peripheral diam.)
int	Internal flow	LP	Angular section with low pressure
ext	External flow	HP	Angular section with high pressure
$total$	Total flow	$\overline{HP}$	Angular range where the displacement chamber is entirely covered by the DP
j	j^{th} control volume		
i	Chamber index	$\overline{LP}$	Angular range where the displacement chamber is entirely covered by the SP
SP, DP	Suction port, Delivery port		